Modulation of Phospholipase A_2: Identification of an Inactive Membrane-Bound State†

W. Richard Burack, Martha E. Gadd, and Rodney L. Biltonen*

Departments of Biochemistry and Pharmacology, University of Virginia Health Sciences Center, Charlottesville, Virginia 22908

Received June 7, 1995; Revised Manuscript Received August 30, 1995®

ABSTRACT: Phospholipase A_2-catalyzed hydrolysis of vesicular phospholipid has been used to model the modulation of an enzyme's function by membrane properties. Phospholipase A_2's (PLA_2) kinetics toward large unilamellar vesicles (LUV) composed of dipalmitoylphosphatidylcholine (DPPC) are anomalous; there is a slow initial phase of catalysis (a lag) which ends abruptly with a sudden increase in the catalytic rate (a burst). The sudden increase in activity is due to the accumulation of a critical mole fraction of reaction product. When the concentration of product exceeds this critical mole fraction, the mixture of reaction products and substrate undergoes compositional phase separation. In this work, we address the molecular details of the coupling between compositional phase separation and activation of PLA_2. A prominent model for this coupling is that compositional phase separation leads to a surface for which PLA_2 has increased affinity, resulting in the recruitment of PLA_2 from solution to the surface. Here, we show that the bulk of PLA_2 is associated with the membrane at a time well before the abrupt increase in catalytic rate. This finding indicates that there must be a relatively inactive, membrane-bound state. Furthermore, PLA_2's kinetics are anomalous even when the substrate comprises a surface to which PLA_2 is bound throughout the time course. With DPPC LUV as the substrate, detailed time courses show that the description of the time course as a lag and a burst is inadequate. Instead, the time course consists of multiple phases of acceleration and deceleration. The data presented here suggest that all these various changes in catalytic rate may be due to product-induced changes in membrane properties. In particular, we suggest that nonequilibrium, microheterogeneities of lipid composition may underlie these very complicated kinetics.

There are several recognized, lipid-derived second-messengers: arachidonic acid and its metabolites, diacylglycerol, lysophosphatidic acid, sphingosine, and ceramides (Liscovitch & Cantley, 1994). While the mechanisms by which these lipid-derived molecules regulate the function of target enzymes remain unclear, two possibilities have frequently been suggested: first, the molecules may act as allosteric effectors at specific sites on the target enzyme; second, the molecules may alter the bulk properties of the membrane in which the target enzyme resides. Although no specific allosteric site for a lipid-derived second-messenger has been identified, the first mechanism is frequently invoked. The second mechanism is also largely speculative. To explore the possible modulatory effects of a membrane's bulk properties on an enzyme, we consider phospholipase A_2 activity toward large unilamellar vesicles.

Several observations suggest that phospholipase A_2 (PLA_2)[1] is sensitive to the phospholipid bilayer's bulk properties. First, op den Kamp et al. observed that the activity of venom and pancreatic PLA_2 toward certain phospholipids is greatest when the reaction temperature is near the substrate's main phase transition temperature (T_m) (1974). Second, the enzyme displays anomalous kinetics that depends on the bulk properties of the membrane substrate. For example, the time course of hydrolysis of dipalmitoylphosphatidylcholine (DPPC) bilayers consists of a prolonged lag phase, which may last hours, during which product only slowly accumulates; eventually, the reaction rate abruptly increases as much as 3 orders of magnitude, a process termed the "burst." The lag phase is shortest at the substrate's T_m, indicating that the substrate's bulk properties affect PLA_2 activity. Third, more recent work shows that the accumulation of a critical amount of the reaction products, fatty acid and lyso-PPC, causes the sudden change in catalytic rate (Apitz-Castro et al., 1982; Burack et al., 1993). The critical mole fraction of reaction product for activation of PLA_2 is also the critical mole fraction for compositional phase separation of products and substrate (Burack et al., 1993).

While the details of the coupling between changes in membrane structure and modulation of PLA_2 activity are unclear, several models have been proposed to explain the connection. [Bell and Biltonen (1992) have collated these models.] A role for membrane charge is often invoked, an idea that hails from early work on PLA_2 and other phospholipases. This proposal stemmed from the observation that the anomalous kinetics were only observed with zwitterionic substrates; with anionic phospholipid vesicles as the substrate, the kinetics were ordinary. More recently, Jain et al. (1989)

† This work was supported by grants from the NIH (GM37658) and NSF (DMB 9005374). W.R.B. was supported by a Medical Scientist Training Grant (5T32 GM07267).

* Author to whom correspondence should be addressed.

® Abstract published in *Advance ACS Abstracts,* November 1, 1995.

[1] Abbreviations: dansyl-DPPE, *N*-[5-(dimethylamino)naphthalene-1-sulfonyl]-1,2- dihexadecanoyl-*sn*-glycero-3-phosphoethanolamine; DPPC, dipalmitoylphosphatidylcholine; DPPG, dipalmitoylphosphatidylglycerol; LUV, large unilamellar vesicle; lyso-PPC, 1-palmitoyl-2-lysophosphatidylcholine; lyso-PPG, 1-palmitoyl-2-lysophosphatidylglycerol; MLV, multilamellar vesicle; PA, palmitic acid; PLA_2, phospholipase A_2; SUV, small unilamellar vesicle; T_m, main phase transition temperature; $X_{dansyl\text{-}DPPE}$, mole fraction of dansyl-DPPE; X_{DPPG}, mole fraction of DPPG.

0006-2960/95/0434-14819$09.00/0

suggested that in zwitterionic vesicles, lateral phase separation segregates the charged fatty acid, which results in a critical charge density necessary to recruit PLA_2 to the membrane surface. This model attributes the burst of activity to the low affinity of PLA_2 for zwitterionic surfaces and its much higher affinity for anionic surfaces. Bell and Biltonen (1992) termed this the "binding-activation" model since it implies that binding of PLA_2 to the membrane surface is the critical step regulating the catalytic rate.

However, compositionally induced changes in surface charge cannot account for all of PLA_2's behavior since manipulations of zwitterionic bilayers, which do not impart an anionic surface charge, activate PLA_2. For example, the catalytic rate toward phosphatidylcholine vesicles can be enhanced by hypertonic shock (Lichtenberg et al., 1986), the addition of lyso-PPC (Bell & Biltonen, 1992; Jain & de Haas, 1983), or the presence of another zwitterionic phospholipid, phosphatidylethanolamine (Sen et al., 1991). We have recently suggested that a common theme that unites all these situations is the presence of highly curved membrane, regardless of surface charge (Burack & Biltonen, 1994). Furthermore, our accumulating data suggest that the compositional phase separation, which occurs in mixtures of substrate and reaction products, is also associated with the induction of regions of high curvature (Burack & Biltonen, 1994). Therefore, the role of surface charge in the activation of PLA_2 remains unresolved.

It remains unclear if association of PLA_2 with the surface is a sufficient condition for rapid catalysis. Here, we dissect binding of PLA_2–membrane association from the PLA_2-catalyzed hydrolysis of the bilayer. These data show that association with the membrane is not sufficient for the development of full activity, that there are multiple surface-associated states, and that these states have distinct catalytic rates and spectroscopic properties. Furthermore, this work describes a frequently overlooked feature of the hydrolysis time course; the time course is not adequately described as a "lag and burst." Specifically, the time course consists of acceleration, followed by deceleration, and then the "burst," which we term the main acceleration. To explain these complicated kinetics, we suggest that the local accumulation of reaction product inhibits PLA_2, such that the kinetics are controlled by the rates of phospholipid and PLA_2 diffusion.

MATERIALS AND METHODS

Materials. All lipids (except palmitic acid) were from Avanti Polar Lipids (Birmingham, AL). Palmitic acid (PA) and the venom of *Agkistrodon piscivorus piscivorus* were obtained from Sigma Chemical Co. (St. Louis, MO). The basic, monomeric, aspartate-49 isozyme of phospholipase A_2 (PLA_2) was purified from the venom according to published procedures (Maraganore et al., 1984). The enzyme concentration was determined from its absorption at 280 nm ($E^{1\%}_{280nm} = 22.0$). Dansyl-DPPE was purchased from Molecular Probes (Eugene, OR).

Lipids: Sample Preparation. All lipids were stored at −20 °C in $CHCl_3$, except for 1:1 (mol/mol) mixtures of PA and 1-palmitoyl-2-lyso-PC (lyso-PPC) which were stored in 1:1 (v/v) $CHCl_3$/MeOH. These lipids formed a flocculent at −20 °C that dissolved when gently heated to 24 °C. To make codispersions, the lipids were mixed in solvent, dried under a stream of N_2, and placed under high vacuum for 8 h. The dried lipids were then hydrated with 60 °C aqueous solution and the temperature was cycled 5 times between room temperature and 60 °C and vortexed periodically. The aqueous solvent contained 50 mM KCl with 10 mM HEPES, pH 8.0, for all studies except activity assays, for which the HEPES was omitted. Large unilamellar vesicles (LUV) were prepared by extruding the lipid dispersion at least 10 times through two 0.1 μm pore size Nucleopore polycarbonate filters using a high-pressure extrusion device from Lipex Biomembranes Inc. (Vancouver, BC) (Hope et al., 1985). The temperature of the lipid dispersion was maintained >50 °C during extrusion. The resulting LUV preparations were characterized by quasi-elastic light scattering using a Nicomp Model 370 submicron particle sizer. The size distribution for most preparations fit well to a Gaussian with an average diameter of 100−120 nm with standard deviations varying from 20 to 40 nm. All lipid preparations were again temperature-cycled 3 times immediately before use and were cooled to the reaction temperature. The [LUV] was calculated assuming 10^5 molecules of phospholipid in each vesicle.

Activity Assay. Product accumulation was monitored with a Radiometer Autoburette in the pH-stat mode as described previously (Burack et al., 1993). A capillary tube fitted to the buret tip, a small-diameter combination electrode, and a thermistor were placed directly into the reaction vessel. The reaction vessel was a quartz cuvette with a cylindrical stir bar. The temperature was stable (±0.05 °C) over several hours. The titrant was 5 or 2.5 mM NaOH in a 50 mM KCl solution. The reaction volume was 2.5 mL, 50 mM KCl, and 5−200 μM $CaCl_2$.[2] The reactions were unbuffered, and the autotitrator was set to maintain the pH at 8.00. Dissolution of atmospheric CO_2 in the reaction vessel contributes to a base line rate of proton release. Base line proton production was recorded for 300−900 s before the addition of PLA_2 to initiate the reaction. The rate of proton production over the 60−300 s immediately prior to the addition of PLA_2 was used as a base line rate of proton production. This base line was subtracted from the titration of PLA_2-catalyzed production of protons.

Throughout this work, we assume that a single proton is released for each molecule of fatty acid produced. The major features of PLA_2's time course were first detected by chromatographic techniques which do not require this assumption (Roholt & Schlamowitz, 1961). Furthermore, the assumption that a titratable proton is produced for each lipid hydrolyzed is key to the interpretation of some of the most extensive quantitative work on PLA_2 activity (Jain & Berg, 1989; Berg et al., 1991). We have confirmed the essential features of the time course by chromatographic techniques which show that under our experimental conditions less than 5% of the total substrate is hydrolyzed prior to the sudden acceleration of catalytic rate (data not shown.) In this work, we do not develop a quantitative model of catalysis; therefore, equating proton titration with fatty acid production is a simplifying, but not an essential, assumption.

Fluorescence Measurements. All fluorescence measurements were made with a T-format SLM 8000C in the slow

[2] The concentration of $CaCl_2$ used with this enzyme is typically 1−20 mM. At these higher concentrations, the sample becomes turbid as product accumulates. We attribute this flocculent to a Ca^{2+}–palmitate salt. Using 5−200 μM $CaCl_2$, no flocculent is apparent. Due to variations in the LUV and PLA_2 preparations, the lag times were frequently difficult to predict. Several calibration experiments were performed with each new batch of reagents. To obtain consistent and convenient lag times, the [Ca^{2+}] was adjusted rather than [PLA_2] or [substrate].

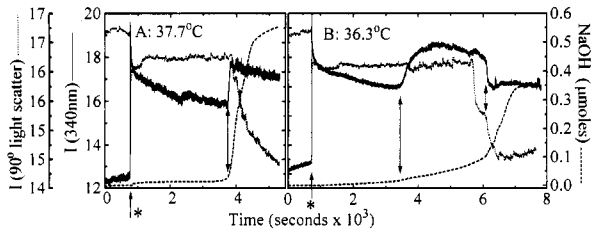

FIGURE 1: Detailed hydrolysis time course for gel-state DPPC LUV. Product accumulation (dashed line), fluorescence intensity (solid line; arbitrary units), and intensity of 90° scattered light (dotted line; arbitrary units) were recorded simultaneously. Reactions were initiated by the addition of PLA_2 at the times marked by the arrows with asterisks. At 37.7 °C, there is good temporal correlation between the increase in fluorescence intensity and the abrupt acceleration of the catalytic rate (solid, double-headed arrow, panel A). At 36.3 °C, the fluorescence increase corresponds to a subtle change in the catalytic rate (solid, double-headed arrow, panel B). The dashed arrow (panel B) shows that the abrupt changes in light scatter and fluorescence are not concomitant. Conditions: 1 mM DPPC (2.5 μmol), 300 nM PLA_2, 50 mM KCl, 20 μM $CaCl_2$, pH 8.0. Excitation = 280 nm, emission = 280 nm (90° light scatter) and 340 nm (fluorescence).

analog mode. Samples were stirred continuously. The temperature of the sample was measured with a calibrated thermistor inserted directly into the cuvette. Temperature was controlled with a circulating water bath (Forma Scientific) and recorded with a resolution of 0.03 °C (Cole-Palmer, digital thermometer 8502-16.)

For studies of PLA_2 intrinsic fluorescence, the excitation and emission wavelengths were 280 nm and 340 nm, respectively; 90° light scatter at 280 nm was recorded simultaneously with all the fluorescence time courses. Energy transfer studies employed dansyl-DPPE as the acceptor. This probe was codispersed in $CHCl_3$ with the phospholipids, and vesicles were prepared as described above. In these experiments, the excitation and emission wavelengths were 280 and 520 nm, respectively.

RESULTS

Detailed Hydrolysis Time Courses. Simultaneous recordings of PLA_2's fluorescence and product accumulation allow correlation between the changes in the intrinsic fluorophores' environment and changes in catalytic rate. Figure 1 shows two time courses below 41.5 °C, the main phase transition (T_m) of the substrate, DPPC LUV. Arrows with asterisks mark the addition of PLA_2, initiating the reaction. Both 1A and 1B depict a slow decay of the initial fluorescence attributable to adherence of PLA_2 to the cuvette. In 1A, there is a sudden increase in the fluorescence at 3750 s that correlates with the abrupt increase in activity (solid arrow, 1A). Bell and Biltonen noted this correlation previously (Bell & Biltonen, 1989a). Since association of PLA_2 with the membrane alters PLA_2's fluorescence, the abrupt increase in fluorescence concomitant with the main acceleration is consistent with the binding activation model.

At 36.3 °C (1B), the correlation between the change in fluorescence and the acceleration of catalytic rate is not so straightforward. The fluorescence increases abruptly during the lag phase, at a time well before the obvious acceleration of product accumulation (solid arrow, 1B). Concomitant with this increase in fluorescence is a subtle but reproducible abrupt change in the hydrolysis rate. About 2500 s later, the main increase in hydrolytic rate is observed, accompanied by a decrease in fluorescence intensity (dashed arrow, 1B). This time course is clearly distinct from that observed at 37.7 °C. These complex kinetics observed at 36.3 °C become even more apparent when the reaction temperature is further below the gel−liquid transition range. Since association with the membrane is thought to be well marked by an increase in protein fluorescence, the data in Figure 1B suggest that during the lag phase, well before the abrupt acceleration of the catalytic rate, PLA_2 is already bound.

In addition to fluorescence and product accumulation, 90° light scatter was also recorded to monitor changes in gross vesicular structure. The intensity of scattered light decreases immediately upon addition of PLA_2, presumably due to absorbance of incident light by the enzyme. In 1A, the light scatter decreases abruptly about 100 s after the sudden increase in fluorescence intensity (solid arrow, 1A). In 1B, the scattered intensity decreases about 100 s before the abrupt decrease in fluorescence and continues to decrease for about 500 s after the fluorescence has stabilized (region of the dashed arrow, 1B). This temporal dissociation of the changes in scattered and fluorescence intensities shows that scattering artifacts do not substantially alter the fluorescence time courses.

Effect of Mole Fraction of DPPG in DPPC LUV on the Association of PLA_2. To further investigate the relationship between binding and catalytic rate, we sought to make a membrane surface to which PLA_2 binds reversibly and for which PLA_2 has a defined affinity. The affinity of PLA_2 for zwitterionic LUV is immeasurably low by our techniques (K_D > 20 mM); no binding to DPPC LUV could be detected using either changes in PLA_2's intrinsic fluorescence or energy transfer techniques at temperatures throughout the phase transition range [although PLA_2's affinity for gel-state DPPC *SUV* is measurable (Bell & Biltonen, 1989b)]. On the other hand, PLA_2 appears to bind irreversibly to vesicles composed entirely of anionic phospholipids. To make a surface for which PLA_2 has an intermediate affinity, we chose to make LUV from a mixture of DPPC and an anionic phospholipid, DPPG. This mixture was chosen because the components have similar main phase transition temperatures and enthalpies, and are thought to mix ideally (Findlay & Barton, 1978). Furthermore, DPPG was selected over a nonhydrolyzable anionic phospholipid analog since the latter could result in the association of PLA_2 with an inhibitor, causing a trivial reason for a lack of correlation between membrane association and catalytic rate.

Changes in PLA_2's intrinsic fluorescence provide a sensitive marker of the enzyme's interaction with membrane and were used to construct binding isotherms (Figure 2). Binding assays were conducted in the presence of excess EGTA, since Ca^{2+} is an essential cofactor for PLA_2. These data show either that PLA_2's affinities for pure DPPC LUV and X_{DPPG} = 0.1 LUV are immeasurably low or that there is no fluorescence change upon association with these LUV. However, PLA_2 has a measurable affinity for X_{DPPG} = 0.2 and X_{DPPG} = 0.5 LUV. The change in fluorescence intensity as a function of phospholipid is saturable for both these populations of LUV, indicating that >95% of the enzyme is bound at high concentrations of lipid. Any attempt to fit these data to a specific model would require assumptions about the size and independence of binding sites. However, without fitting, it is still possible to place upper limits on the dissociation constants (K_D): the maximum possible K_D for association with X_{DPPG} = 0.2 LUV is 50 μM while that for X_{DPPG} = 0.5 LUV is 2.5 μM. Since in the limit of high

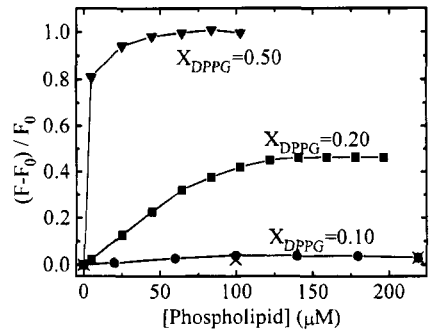

FIGURE 2: Binding of PLA_2 to DPPG/DPPC LUV. The change in PLA_2's intrinsic fluorescence was used to construct binding isotherms. F_0 is the fluorescence of PLA_2 prior to the addition of phospholipid. Triangles, $X_{DPPG} = 0.5$; squares, $X_{DPPG} = 0.2$; circles, $X_{DPPG} = 0.1$; crosses, $X_{DPPG} = 0$. [PLA_2] = 300 nm, 50 mM KCl, 1 mM EGTA, 10 mM HEPES, pH 8.0, 35 °C.

[lipid], the surface concentration of PLA_2 approaches one molecule per vesicle, these data also indicate that the change in fluorescence intensity upon association with these membranes depends on X_{DPPG}.

There are two critical reasons to document the reversibility of association. First, [PLA_2] multiplied by a reasonable estimation of the number of lipid molecules in a binding site yields a value within an order of magnitude of the K_D. (The [PLA_2] could not be lowered since the assay relies on the enzyme's fluorescence.) Under these conditions, it may be difficult to distinguish the isotherms for a reversible association from irreversible stoichiometric interaction of PLA_2 and DPPG. Showing reversibility resolves this question. Second, studying reversibility yields information about the enzyme's off-rate from these surfaces, with implications for the residence time on a surface.

The reversibility of PLA_2 binding to LUV of equimolar DPPC:DPPG ratio ($X_{DPPG} = 0.5$) at 36 °C was determined using a probe (dansyl-DPPE) for fluorescence energy transfer studies. The difference of the excitation spectra of these labeled vesicles ($X_{dansyl\text{-}DPPE} = 0.02$) with and without PLA_2 contains one peak at 280 nm, corresponding to the excitation spectrum of PLA_2 (data not shown). Therefore, the change in the dansyl emission intensity is due to a change in the energy transfer from PLA_2's fluorescent residues.

To determine the reversibility of PLA_2 binding, the enzyme was first incubated with dansyl-labeled vesicles, and the increased fluorescence intensity indicated the association of PLA_2 with these vesicles (Figure 3). The concentration of phospholipid was more than 20 times the maximum possible K_D to ensure >95% of the PLA_2 was bound. While exciting PLA_2 at 280 nm and recording dansyl emission at 510 nm, a concentrated solution of LUV with $X_{DPPG} = 0.5$ was added to increase the total concentration of lipid by a factor of 5 (arrow at 0 s). The dansyl emission intensity decayed to 0.2 of the peak value, indicating that PLA_2 had distributed among all the vesicles. Similar results were obtained using $X_{DPPG} = 0.2/X_{dansyl\text{-}DPPE} = 0.02$ LUV, but the decay of fluorescence occurred in less than 2 s (data not shown). No energy transfer was apparent with $X_{DPPG} = 0.1/X_{dansyl\text{-}DPPE} = 0.02$ LUV. These findings corroborate those in Figure 2; the binding is reversible, and the affinity increases with the mole fraction of the anionic component.

The Role of Anionic Surface Charge in Determining the Complex Kinetics. The accumulation of a critical mole fraction of reaction product somehow triggers the abrupt acceleration seen in Figure 1A. The binding−activation

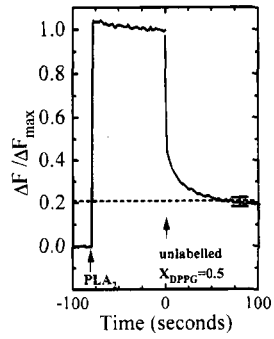

FIGURE 3: PLA_2 association with $X_{DPPG} = 0.5$ LUV is rapidly reversible. 50 μM phospholipid was presented as $X_{DPPG} = 0.5$ LUV containing $X_{dansyl\text{-}DPPE} = 0.02$. 300 nM PLA_2 was added at the first arrow. The dansyl fluorescence was allowed to stabilize for 75 s, and 200 μM phospholipid as $X_{DPPG} = 0.5$ LUV was added at the second arrow. The horizontal dashed line at 0.2 is the expected relative fluorescence intensity if the PLA_2 distributed evenly among all the vesicles. The vertical error bar represents the mean and standard deviation for four experiments. 50 mM KCl, 10 mM HEPES, pH 8.0, 1 mM EGTA, 36 °C. Excitation = 280 nm, emission = 510 nm.

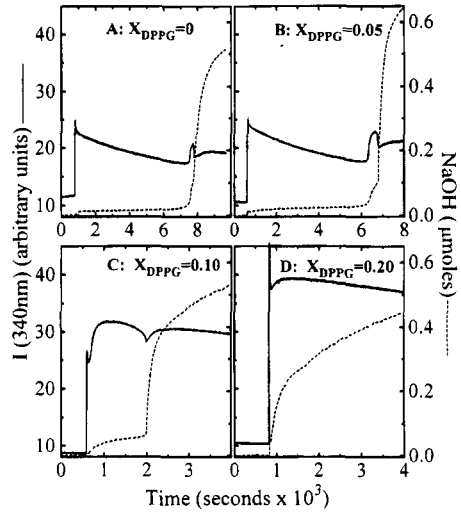

FIGURE 4: Effect of the mole fraction of DPPG on the complex time courses. Product accumulation (dashed lines) and intrinsic fluorescence (solid lines) were recorded simultaneously. The reaction was initiated with addition of PLA_2 at about 750 s (marked by the abrupt increase in observed fluorescence). [PLA_2] = 300 nm, 1 mM phospholipid (2.5 μmol), 50 mM KCl, 20 μM $CaCl_2$, 10 μM EGTA, 10 mM HEPES, pH 8.0, 36.5 °C.

model suggests that the negatively charged product, PA, is responsible for the acceleration. Within this context, DPPG is a substitute for PA. The dependence of the time courses' details on the degree of binding was studied using the LUV for which the enzyme's affinities were examined above. Since the affinities for $X_{DPPG} = 0.2$ and $X_{DPPG} = 0.1$ LUV are so different, the fractions of PLA_2 bound to these surfaces in the presence of 1 mM phospholipid are >95% and <5%, respectively. Figure 4 shows the hydrolysis time courses at 36.5 °C (gel state) with 1 mM substrate, presented as DPPC LUV or LUV made from binary mixtures of DPPC and DPPG. Note that the addition of DPPG reduces the lag time. With $X_{DPPG} = 0.2$, the lag time is no longer apparent.

The complex kinetics seen in Figure 1B are clearly reproduced in Figure 4A,B. Details of these Figures show the part of the time course that ends the lag phase (Figure 5). Both with $X_{DPPG} = 0$ and with $X_{DPPG} = 0.05$, there is an obvious increase in the catalytic rate that corresponds to the increase in PLA_2's fluorescence. There is also a second

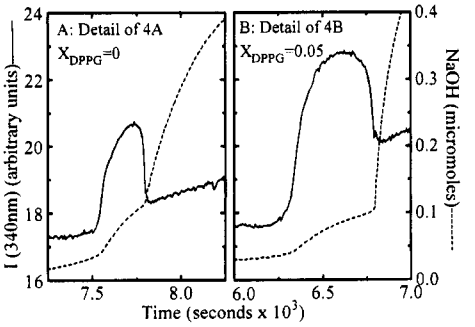

FIGURE 5: Correlation of changes in the fluorescence intensity and changes in the catalytic rate. Panels A and B are details of panels A and B of Figure 4, respectively.

abrupt increase in the catalytic rate that correlates well with a decrease in PLA_2's fluorescence. We term these highly reproducible events the initial acceleration (the first increase in rate) and the main acceleration (the second increase in rate).

Two features of the time courses change systematically as X_{DPPG} increases from 0 to 0.1 (Figure 4A−C). First, the lag period shortens with increasing X_{DPPG}. Second, the initial acceleration moves to earlier times and is temporally better separated from the main acceleration. When $X_{DPPG} = 0.10$, the initial acceleration occurs shortly after addition of PLA_2, but more than 1000 s before the main acceleration.

There are two aspects of the time courses that do not vary as X_{DPPG} varies from 0 to 0.1. First, the fluorescence intensity increases during the initial acceleration and decreases at the main acceleration. Second, the extent of product accumulation that occurs up to the time at which the main acceleration begins is similar regardless of the X_{DPPG}. This result implies that the complex kinetics cannot be due to the preferential hydrolysis of DPPG.

Complex Kinetics Occur Even When All PLA_2 Is Initially Bound. The simple kinetics under conditions when all the enzyme is associated with the membrane at the initial time are consistent with the binding−activation model (Figure 4D). However, the various phases of the time courses are compressed into shorter total time as X_{DPPG} increases, thereby suggesting that these complexities may still be present on $X_{DPPG} = 0.2$ LUV but poorly resolved. The lag phase for hydrolysis of DPPC LUV is the time required to accumulate a critical mole fraction of reaction product. Therefore, the length of the lag should be increased by decreasing the enzyme concentration, decreasing the concentration of Ca^{2+}, or increasing the phospholipid concentration. Indeed, such manipulations prolonged the time course, revealing additional complexities that occur during the hydrolysis of $X_{DPPG} = 0.2$ LUV.

As in Figure 4D, the experiment shown in Figure 6 uses $X_{DPPG} = 0.2$ LUV as substrate. In Figure 6, the time course is prolonged by lowering the concentration of the essential cofactor, Ca^{2+} (compare panels A and B), and then further prolonging the time course by increasing the concentration of substrate (compare panels B and C). Again, product accumulation and intrinsic fluorescence of PLA_2 were recorded simultaneously. Upon increasing the length of the time course, a period of relatively rapid proton release immediately after the addition of PLA_2 becomes apparent. This immediate phase of proton release slows, and only then does a lag phase begin. The protons released in the immediate phase of rapid catalysis account for no more than

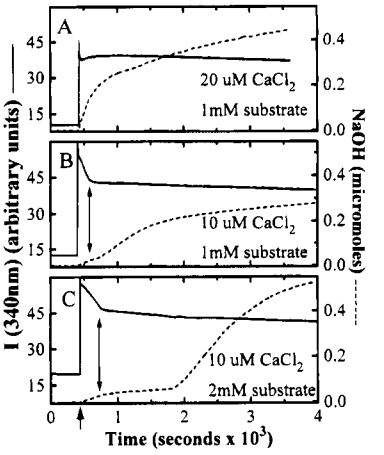

FIGURE 6: Induction of complex kinetics in the hydrolysis of X_{DPPG} = 0.2 LUV. Product accumulation (dashed lines) and intrinsic fluorescence (solid lines) were recorded simultaneously. Reaction conditions are as in Figure 4. The data in Figure 4D are shown again in Figure 6A (time axis is offset to allow direct comparison of the three panels). [Phospholipid] = 1 mM (2.5 μmol) in panels A and B, and 2 mM (5 μmol) in panel C. [$CaCl_2$] = 20 μM in panel A, and 10 μM in panels C and B. In all panels, [PLA_2] = 300 nM, 50 mM KCl, 10 μM EGTA, 10 mM HEPES, pH 8.0, 36.5 °C. In panels B and C, the vertical arrows show the correlation between the stabilization of the fluorescence intensity and the end of the initial phase of rapid hydrolysis.

2−4% of the available substrate in the outer monolayer. This amount is comparable to that accumulated during the initial acceleration phases in Figure 4A−C. By increasing the length of the time course, the hydrolysis of $X_{DPPG} = 0.2$ LUV appears qualitatively similar to that for $X_{DPPG} = 0.1$ LUV in Figure 4C.

The fluorescence time courses in Figure 6B,C show that the state of PLA_2 changes during the initial period of rapid hydrolysis. The peak fluorescence occurs immediately after the addition of PLA_2 and decays as the rate of the initial rapid proton release slows. When the rapid proton release ends, the fluorescence becomes stable. Furthermore, PLA_2's fluorescence does not change at the time of the main acceleration. This finding suggests that the local environment of PLA_2's fluorescent residues does not change dramatically at the main acceleration on $X_{DPPG} = 0.2$ LUV. The simultaneous recordings of the 90° light scatter indicate that the observed fluorescence intensities in these experiments are not affected by changes in the light scatter (data not shown).

The hydrolysis time courses contain no abrupt change that clearly defines the end of what we have termed the "initial phase of rapid hydrolysis". The catalytic rate decreases throughout this phase and appears to reach a relatively fixed value at the time that the fluorescence also stabilizes (Figure 6B,C). Thus, we define the "initial phase of rapid hydrolysis" as starting with the initiation of the reaction and ending when the catalytic rate and fluorescence stabilize.

Past analyses of PLA_2-catalyzed hydrolysis of DPPC LUV have largely assumed that the catalytic rate increased monotonically. The data in Figures 1B and 4A show that this is not so; the rate increases, slows, and then increases again. Figure 4 shows that the addition of an anionic phospholipid alters the temporal relationship between these processes. Since anionic charge increases association of PLA_2 with the membrane, we hypothesize that DPPG plays one of palmitic acid's putative roles, namely, recruiting PLA_2 to the membrane. After the accumulation of a small amount

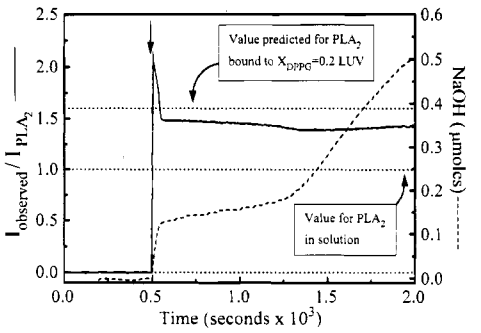

FIGURE 7: Little PLA_2 is free in solution at any time during the hydrolysis of $X_{DPPG} = 0.2$ LUV. Product accumulation (dashed line) and the intrinsic fluorescence of PLA_2 relative to the fluorescence of PLA_2 in the absence of phospholipid (solid line, $I_{observed}/I_{PLA_2}$) were recorded simultaneously. The reaction was initiated with addition of PLA_2 at the arrow. I_{PLA_2} is the fluorescence of 300 nM PLA_2 in the absence of phospholipid. The horizontal line at 1.6 is the relative fluorescence observed for PLA_2 in the presence of 1 mM phospholipid presented as $X_{DPPG} = 0.2$ LUV. This value was determined by an experiment as in Figure 2 ($n = 5$, SD = 0.04). $[PLA_2] = 300$ nM, 2 mM phospholipid (5 μmol), 50 mM KCl, 40 μM $CaCl_2$, 20 μM EGTA, pH 8.0, 36.5 °C.

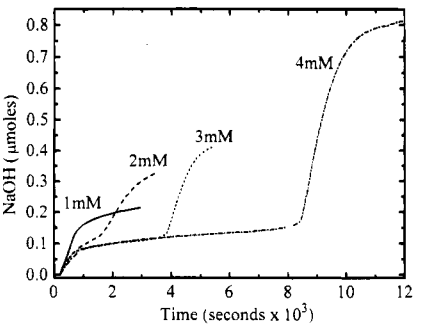

FIGURE 8: Extent of product accumulation in the initial phase of rapid hydrolysis does not depend on the concentration of $X_{DPPG} = 0.2$ LUV. The reactions were initiated with addition of PLA_2 at 300 s. $[PLA_2] = 600$ nM, phospholipid presented as $X_{DPPG} = 0.2$ LUV (1 mM = 2.5 μmol; 2 mM = 5 μmol; 3 mM = 7.5 μmol; 4 mM = 10 μmol), 50 mM KCl, 16 μM $CaCl_2$, 10 μM EGTA, pH 8.0, 36.7 °C.

of reaction product, the catalytic rate toward both DPPC and $X_{DPPG} = 0.2$ LUV slows. To investigate the basis for this deceleration, we focus on the $X_{DPPG} = 0.2$ LUV rather than DPPC LUV since the extremely long and subtle time courses with the latter as substrate precluded extensive analysis.

PLA_2 Is Associated with the Membrane throughout the Complex Time Course. The data above show that the initial phase of rapid hydrolysis of $X_{DPPG} = 0.2$ LUV is accompanied by a high fluorescence state of PLA_2. We considered that the profound slowing of the catalytic rate could be caused by dissociation of PLA_2 from the vesicles, which could also explain the simultaneous decay of the fluorescence intensity. However, Figure 7 shows that the fluorescence intensity during the period between the initial phase of rapid hydrolysis and the main acceleration is similar to that of membrane-associated PLA_2. Furthermore, the fluorescence intensity does not change at the main acceleration. If the rate enhancement at the main acceleration were due to recruitment of PLA_2 to the surface, then the fluorescence of PLA_2 should have increased. These data suggest that very little PLA_2 is in solution during the period between the initial phase of rapid hydrolysis and the main acceleration.

Characterization of the Initial Phase of Rapid Hydrolysis. The rate of the initial phase of hydrolysis displays those characteristics expected of an enzymatically catalyzed reaction: the rate is directly proportional to the $[PLA_2]$ and $[Ca^{2+}]$ (5−50 μM, data not shown). The durations of the initial phase of rapid hydrolysis and the initial high fluorescence phase are both prolonged by lowering either $[PLA_2]$ or $[Ca^{2+}]$ (data not shown). Furthermore, when PLA_2 is added to $X_{DPPG} = 0.2$ LUV in the absence of Ca^{2+}, the fluorescence is immediately stable at a value expected for membrane-associated PLA_2. With subsequent addition of Ca^{2+}(4 μM), there is an initial period of rapid hydrolysis and the fluorescence decays to a stable value as that hydrolysis slows (data not shown). These data indicate that the fluorescence time course is a reliable indicator of whatever events underlie the initial rapid phase of hydrolysis.

The PLA_2:LUV ratio determines how $[PLA_2]$, [LUV], and $[Ca^{2+}]$ affect the amount of product which accumulates in the initial phase of rapid hydrolysis. In all the experiments described thus far, the $[PLA_2]$ was sufficient to provide a spectroscopic signal. Under these conditions, there are 15−30 molecules of PLA_2 on each vesicle (i.e., PLA_2/LUV > 1). With PLA_2/LUV > 1, the extent of hydrolysis in the initial phase is weakly dependent on $[PLA_2]$ (see below), weakly dependent on $[Ca^{2+}]$ (5−50 μM, data not shown), but independent of the [phospholipid] presented as $X_{DPPG} = 0.2$ LUV (Figure 8). This last result shows that the initial phase of rapid hydrolysis is not due to the preferential hydrolysis of a fixed fraction of the phospholipid or contaminant. Furthermore, these data reproduce the phenomenon shown in Figure 6: complex kinetics can be induced by increasing the concentration of substrate.

The slowing of the initially rapid catalysis could be due to the accumulation of reaction product, which could in some way retard catalysis. This effect of product could be due to product inhibition, substrate depletion, or both. If inhibition by product is responsible for the slowing of the catalytic rate, then the addition of reaction products to virgin LUV should abolish the initial rapid phase of catalysis. Reaction products consisting of 1:1 palmitic acid/lyso-PPC or 1:1 palmitic acid/lyso-PPG were added to $X_{DPPG} = 0.2$ LUV. Similar results were obtained in both cases. While 5 mol % reaction products markedly decreased the time before the main acceleration, there was no perceptible effect on the initial rapid phase of catalysis (data not shown). The addition of 10 mol % reaction products, which is sufficient to induce compositional phase separation in the DPPC/PA/lyso-PC system (Burack et al., 1993), abolished the complex kinetics.

If the effect of product accumulation is manifest only in the small region of the membrane near an active enzyme, then the extent of product accumulation in the initial rapid phase of hydrolysis will depend on the density of PLA_2 on the membrane. For example, an active molecule of PLA_2 which remained at a fixed location on the membrane might be totally surrounded by its own product while the entire membrane is only a few percent hydrolyzed. A neighboring molecule of PLA_2 would also experience a high concentration of product. When the surface density of PLA_2 is sufficiently large (i.e., PLA_2/LUV > 1, as in all the experiments presented thus far), the model predicts that there will be cooperative inhibition. This cooperative inhibition will cause the extent of product accumulation in the initial phase to increase less than linearly with the $[PLA_2]$. The model further predicts that when PLA_2/LUV < 1 each molecule of PLA_2 will act independently so that the extent of product

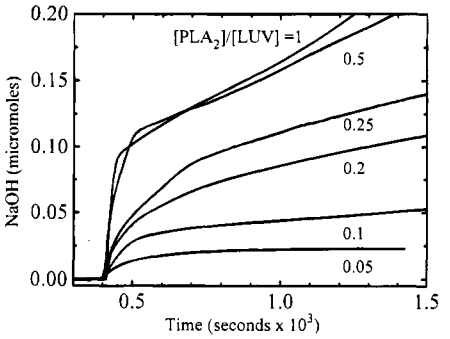

FIGURE 9: Ratio of PLA_2/LUV (X_{DPPG} = 0.2 LUV) affects the relationship between [PLA_2] and the extent of product accumulation in the initial phase of rapid hydrolysis. PLA_2/LUV was altered by varying the [PLA_2] at a fixed concentration of LUV. The number of LUV was calculated assuming 10^5 molecules of phospholipid in each LUV (100 nm diameter). Assay conditions: 50 mM KCl, 10 μM EGTA, [$CaCl_2$] = 200 μM, [phospholipid] = 5 mM (12.5 μmol), 36 °C, [PLA_2] = 2.5, 5, 10, 12.5, 37.5, 50, or 140 nM. (Due to low catalytic rates and base line drifts, reproducible rates at the lowest [PLA_2] could be obtained only by increasing the [$CaCl_2$]. Even with the increased [$CaCl_2$], the lag time with the four lower concentrations of PLA_2 was >1.5 h, so the experiment was stopped before an abrupt acceleration was observed.)

accumulation in the initial phase will vary linearly with the [PLA_2].

Figure 9 shows that the product accumulation in the initial phase varies linearly with [PLA_2] when PLA_2/LUV < 1 but not when PLA_2/LUV $\approx$ 1. Assuming that there are 10^5 phospholipid molecules in each LUV, a ratio of PLA_2 to LUV can be calculated. The concentration of substrate is the same in all seven time courses shown in Figure 9, but the [PLA_2] is varied to obtain the calculated PLA_2/LUV ratio. These data show that when PLA_2/LUV < 1, the amount of product which accumulates in the initial phase of rapid hydrolysis varies linearly with the [PLA_2] (compare the time courses with the lowest ratios between 0.05 and 0.25). Furthermore, [LUV] and [Ca^{2+}] alter the extent of hydrolysis (data not shown). However, as PLA_2/LUV approaches 1, the relationship between [PLA_2] and the extent of product accumulation in the initial phase of rapid hydrolysis is no longer linear. Raising the PLA_2/LUV approximately 300% (from 1 to 2.8) increases the extent of hydrolysis in the initial rapid phase by only 25%.

Complex Reaction Time Courses Are More Difficult To Induce with Liquid-Crystalline X_{DPPG} = 0.2 LUV. The experiments above suggest that the function of PLA_2 may be limited by locally accumulated reaction product. The slowing of the catalytic rate may be due to poor diffusion of product away from (or substrate to) a membrane-bound molecule of PLA_2. Lateral diffusion rates of phospholipids in gel and liquid-crystalline states differ by several orders of magnitude (Marsh, 1990). If slow lateral diffusion causes the anomalous time courses, then the use of liquid-crystalline substrate should produce relatively simple time courses. Figure 10 shows the time course of hydrolysis of X_{DPPG} = 0.2 LUV at 36.5 and 45 °C. The time course of hydrolysis above the phase transition appears considerably simpler than that obtained with gel state substrate. The lag time is nondetectable and at least 2 orders of magnitude shorter. Attempts to induce a lag by doubling the [phospholipid] had no appreciable effect at 45 °C while at 36.5 °C the lag time was >7200 s (data not shown).

A Nomenclature for Describing the Complex Kinetics. Given the observation of such complicated kinetics, division

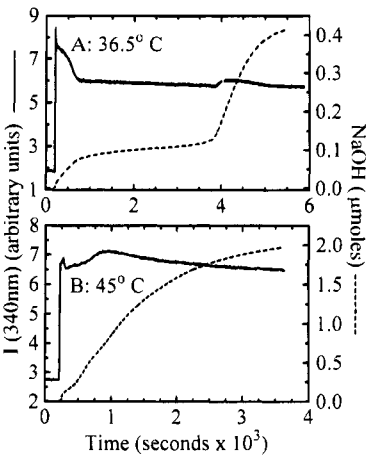

FIGURE 10: Complex time courses are not apparent with liquid-crystalline X_{DPPG} = 0.2 LUV. Product accumulation (dashed lines), intrinsic fluorescence (solid lines), and 90° light scatter (data not shown) were recorded simultaneously. Panel A is at 36.5 °C and panel B at 45 °C. The reaction was initiated with addition of PLA_2 at the times marked by the abrupt increase in the observed fluorescence. [PLA_2] = 600 nM, [phospholipid] = 2 mM (5 μmol), 50 mM KCl, 16 μM $CaCl_2$, 10 μM EGTA, 10 mM HEPES, pH 8.0.

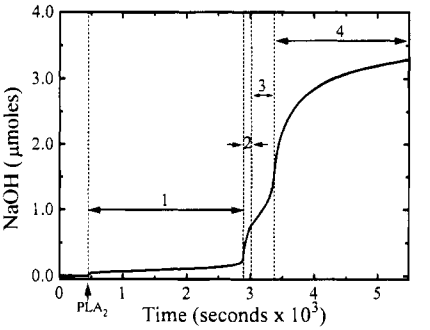

FIGURE 11: Using points of inflection to parse a hydrolysis time course for gel-state DPPC LUV. Each vertical dotted line passes through a point of inflection in the product accumulation time course. The numbers correspond to the four phases of hydrolysis described under Discussion. 1, initial acceleration; 2, initial deceleration; 3, main acceleration; 4, terminal deceleration. Conditions: [PLA_2] = 1.5 μM, [DPPC] = 10 mM (25 μmol), 50 mM KCl, 10 μM EGTA, 20 μM $CaCl_2$, pH 8.0, 36.7 °C.

of the time course simply into lag and burst periods is not adequate. There are processes that activate and others that inhibit PLA_2. When activation predominates, the catalytic rate increases, while the opposite is true when an inhibitory process predominates. These phases are then termed acceleration and deceleration phases, respectively. An inflection point occurs when the magnitudes of activating and inhibitory processes are equal. These points divide the time courses into discrete phases during which either activation or inhibition predominates. Figure 11 shows a parsing of a time course for hydrolysis of gel-state DPPC LUV into four distinct phases: initial acceleration, then deceleration, then the main acceleration, and finally terminal deceleration. Applying the same analysis to other time courses, the data in Figure 6C consist of three phases: initial deceleration, followed by acceleration, and then terminal deceleration.

DISCUSSION

Binding and Activity Are Dissociable. The results presented here show that the binding of PLA_2 to the surface is not sufficient for PLA_2 to manifest full activity. To dissect

the anomalous kinetics, first consider conditions under which no hydrolysis occurs. The fluorescence change upon association with membrane depends on the phospholipid composition (Figure 2). Ghomaschi et al. (1991) noted this phenomenon but ascribed it no significance. This simple result has an important implication: varying the composition affects the nature of the bound state. Therefore, changes in the fluorescence of PLA_2 during the time course of hydrolysis may reflect changes in the bound state rather than merely association or dissociation from the membrane. Next, consider Figures 6−8 in which the substrate is $X_{DPPG} = 0.2$ LUV. In these experiments, >95% of the PLA_2 is bound initially, and the bulk of the enzyme remains membrane-associated throughout the time course. The occurrence of complex kinetics under these conditions requires at least two kinds of membrane bound states: one with low activity and one with high activity.

The Observation of Complex Kinetics. The experiments presented here show an extremely reproducible initial phase of rapid hydrolysis when $X_{DPPG} = 0.2$ LUV is the substrate. Furthermore, this initial phase of rapid hydrolysis has a cognate process in the hydrolysis of DPPC LUV. These complexities in the time courses have been frequently overlooked for several reasons. First, the extent of product accumulation in the initial phase is small, usually accounting for less than 3% of the total substrate. Second, these additional complexities in the time course only become apparent when the lag period is on the scale of hours. To attain such conditions, the $[Ca^{2+}]$ is 3 orders of magnitude lower than that frequently used, the concentration of substrate is higher than in previous studies, and the temperature is further from the main phase transition (Bell & Biltonen, 1989a). Third, the initial acceleration would be almost indistinguishable from the main acceleration if the temporal resolution of the product titration were any less than that obtained here (Figure 4A and its detail, Figure 5A). For example, with a significant loss of time resolution, the titration data in Figure 4A might seem consistent with the kinds of continuous activation models that have been considered previously (Romero et al., 1987; Bell & Biltonen, 1992; Verger et al., 1973; Jain & Apitz-Castro, 1978). Interfacing the automatic buret with a personal computer increased the temporal resolution by a factor of 1000 compared to previous studies in which the data were recorded on a strip chart. Fourth, the correlation of a spectroscopic change with the initial acceleration has allowed even subtle changes in the base line rate to be identified as the initial acceleration. For example, Figure 1B shows an abrupt change in PLA_2's fluorescence approximately 2200 s before the main acceleration. Noting this early change in the spectroscopic properties, it is then possible to detect a simultaneous distinct change in the catalytic rate. Without the spectroscopic observable, this change in rate would have gone unnoticed.

We are unaware of previous reports that describe the time course for hydrolysis of DPPC LUV shown here (i.e., one that includes at least two acceleration phases). However, there are several reports of time courses that begin with rapid hydrolysis and then slow (similar to those shown in Figure 6B,C for the hydrolysis of $X_{DPPG} = 0.2$ LUV) using either DPPC SUV or DPPC MLV as the substrate. The period of high initial activity is explicitly examined in several publications (Upreti & Jain, 1980; Apitz-Castro et al., 1982; Tinker & Wei, 1979; Tinker et al., 1978) and is noticeable in others (Fernandez et al., 1991a,b). Upreti and Jain (1980) suggested that the membranes contained preexisting defects that were preferential sites of hydrolysis. Menashe et al. (1986) found this phenomenon difficult to reproduce and suggested that the initial rapid phase of hydrolysis was an experimental artifact due to the use of a pH-stat to monitor activity. We can reproduce these results only when the substrate is made by resuspending dried DPPC in aqueous solvent below that lipid's T_m (unpublished data). These conditions are likely to produce lamellae that are riddled with defects. However, using our standard preparation of DPPC LUV, an initial rapid phase of hydrolysis is not observed.

The Origin of the Complex Time Courses of Hydrolysis of Gel-State Substrates. The presence of the immediate phase of rapid hydrolysis suggests that PLA_2 is relatively active toward $X_{DPPG} = 0.2$ LUV, requiring no slow conformational change, covalent modification, or slow insertion into the membrane. This initial activity soon decays to a rate less than 5% of the initial rate when less than 4% of the available substrate is hydrolyzed. To exert this large effect at such a low concentration, either the reaction product must bind with high affinity to PLA_2 or it must be inhomogeneously distributed such that PLA_2 is in contact with regions that are enriched in reaction product. Two results suggest that reaction product does not act as a high-affinity inhibitor: first, the existence of the main acceleration in the presence of greater amounts of product; second, the products' putative inhibitory effect could not be mimicked by codispersing reaction product with the substrate. Inhomogeneous distribution of reaction products could be either the equilibrium disposition of the products or the result of slow diffusion of product away from regions where hydrolysis has occurred. Again, codispersions including small amounts of reaction product did not abolish the initial rapid phase of hydrolysis. Assuming that codispersions are at equilibrium, this result suggests that the equilibrium distribution of reaction products is not sufficient to induce the decay in the catalytic rate.

Three results suggest that limitations on lateral diffusion of PLA_2 or reaction products may underlie the complex kinetics. First, the severe temperature dependence of the complex kinetics suggests a role for proximity to the main phase transition in relieving the inhibition (compare the kinetics at 37.7 and 36.3 °C in Figure 1A,B). Since the lateral diffusion coefficients are at least 3 orders of magnitude greater in the liquid state than in the gel state, a small fraction of liquid lipid may be sufficient to dramatically alter the lifetimes of product-enriched clusters. Second, the complex kinetics characterized in gel substrate are not readily apparent with liquid-crystalline substrate where diffusion rates are orders of magnitude greater (Figure 10). Third, the effect of PLA_2's surface density on product accumulation in the initial phase of rapid hydrolysis (Figure 9) suggests a role for the local accumulation of product.

The data presented in Figure 9 are reminiscent of those presented by Jain et al. (1986b). Using SUV composed of an anionic phospholipid, dimyristoylphosphatidylmethanol, these workers observed that the dependence of the amount of product accumulation on the $[PLA_2]$ was determined by the PLA_2/SUV; with $PLA_2/SUV < 1$, there was a linear dependence, but with $PLA_2/SUV > 1$, the amount of product accumulation did not change substantially as the $[PLA_2]$ was raised. They concluded that each enzyme bound tightly to a vesicle and catalyzed the complete hydrolysis of the outer

monolayer, and that the vesicles remained intact even after complete hydrolysis of the outer monolayer. Given the apparent linear relationship between [PLA_2] and the amount of product which accumulates, these authors calculated the proportionality coefficient of 4500. This number was also the estimated number of phospholipid molecules in the outer monolayer of the SUV. This concordance formed the basis of their suggestion that each PLA_2 molecule bound a single vesicle and hydrolyzed the entire outer monolayer in a highly processive manner (the "scooting mode"). Analyzing the extent of product accumulation in the initial rapid catalytic phase (Figure 9), we arrive at similar a proportionality constant (4000−5000) despite the use of LUV which contain approximately 50×10^3 phospholipids in the outer monolayer. Since we find no correlation between the proportionality constant and the number of lipids in the outer monolayer, we have chosen to explain our results in terms of local inhibition attributable to product clustering and the enzyme's putative slow dissociation from these product-enriched regions.

There is evidence for the nonequilibrium distribution of reaction products and its effects on rate. First, the fluorescence of a membrane probe continues to change for minutes after PLA_2's catalysis is quenched during the main acceleration (Burack et al., 1993). This result shows that during hydrolysis the membrane is not in an equilibrium state. Second, as the catalytic rate toward DPPC SUV is increased by increasing [Ca^{2+}], there is an increase in a synergistic effect of Mg^{2+} (Lathrop & Biltonen, 1992). Lathrop and Biltonen suggested that at lower catalytic rates the diffusion of PLA_2 and products was sufficiently fast to alleviate local product inhibition. However, at higher catalytic rates, product inhibition occurred. Mg^{2+} might relieve the inhibition by disrupting the electrostatic interactions between PLA_2 and PA, thus limiting the formation of product−PLA_2 clusters.

The role of surface charge is underscored by the dependence of both PLA_2's affinity for membrane and the intrinsic fluorescence on X_{DPPG} (Figure 2). PLA_2's affinity for LUV appears to have a cooperative dependence on X_{DPPG}; the K_D for $X_{DPPG} = 0.1$ LUV is >20 mM, but <50 μM for $X_{DPPG} = 0.2$ LUV. Given this cooperative interaction, it seems likely that PLA_2 could either induce lateral phase separation of anionic lipids within the plane of the bilayer or increase the lifetime of nonequilibrium clusters of anionic product. Such preferential association of PLA_2 with discrete regions would suggest that PLA_2 is also enriched or even aggregated on those small regions.

The magnitude of the fluorescence change upon association also shows a nontrivial dependence on X_{DPPG}. Data presented elsewhere show that the fluorescence change upon association with DPPG/DPPC LUV is maximal for $0.5 < X_{DPPG} < 1.0$ (Burack & Biltonen, 1994). Since no local enrichment of anionic lipid is possible for $X_{DPPG} = 1.0$ LUV, we hypothesize that aggregation of PLA_2 is also less likely here than on surfaces composed only partially of DPPG. Therefore, we suggest that the fluorescence change upon association with the membrane may in part reflect PLA_2's degree of aggregation on the membrane.

To understand how the combination of surface charge, limits on lateral diffusion, compositional phase separation, and possibly aggregation of PLA_2 produces complex kinetics, consider the time courses for hydrolysis of gel-state DPPC LUV (Figure 11). Initially, little PLA_2 is associated with the surface, resulting in low catalytic rates. As palmitic acid accumulates, PLA_2 is recruited to the surface, and the catalytic rate increases; this charge-induced binding accounts for the initial acceleration. As the charge increases, the enzyme's off-rate from a particular site on the membrane decreases, thereby trapping the enzyme in a local pool of product. Thus, a combination of a high affinity of PLA_2 for anionic sites and poor lateral diffusion of lipids is invoked to account for the deceleration. This model predicts that PLA_2 will tend to aggregate at the end of the initial deceleration, accounting for the cooperative inhibition (Figure 9). In fact, Grainger et al. used fluorescence microscopy to show that PLA_2 aggregates during hydrolysis of a monolayer at its gel−liquid-crystalline transition (1990, 1989). Continued slow accumulation of reaction products eventually causes a compositional phase separation of the lipid components. This phase separation is accompanied by a large-scale change in vesicular structure (Burack et al., 1994; Burack & Biltonen, 1994). Presumably, these phase and structural changes somehow mitigate the product-induced inhibition, perhaps disrupting product clusters.

It must be emphasized that the change in vesicular structure accompanying phase separation of reaction products appears to relieve product-related inhibition. For inhibition to occur, we suggest that diffusion of the enzyme and product must be slower than the intrinsic turnover number. In fluid state $X_{DPPG} = 0.2$ LUV where lateral diffusion is rapid, no inhibition is observed. In the other cases, diffusion limitations (hence inhibition of PLA_2) may be relieved by dynamic structural changes, such as those induced by osmotic shock or compositional phase separation. The packing defects which accompany these structural changes may allow a dramatic increase in the translational diffusion of lipid and enzyme (Derzko & Jacobson, 1980). [Others have suggested that a critical mole fraction of a second component may percolate, enhancing diffusion by a mechanism which does not involve defect formation (Smaby et al., 1994; Thompson et al., 1992).]

The complexity of the observed time course depends on the initial state of the bilayer and the temporal relationship among the accelerating and decelerating processes. For example, using $X_{DPPG} = 0.2$ LUV at 36.5 °C, all PLA_2 is bound at the initial time point so that the initial acceleration process is not observed (Figure 6B,C). These time courses begin with a deceleration phase. Using DPPC LUV at 37.7 °C, a larger fraction of the lipid is in the fluid phase, presumably enough to allow significantly greater lateral diffusion rates (Figure 1A). Under these conditions, clusters of anionic products may have only very short lifetimes so that local inhibition does not occur. Therefore, this time course lacks a deceleration phase. This framework provides a series of testable hypotheses concerning the effects of membrane properties on PLA_2's activity.

Models and More Models. It has been 20 years since Op den Kamp et al. noted the anomalous reaction kinetics of PLA_2 and suggested that defects in the membrane surface affected activation (op den Kamp et al., 1975). Other models of membrane structure's role in activating PLA_2 do not invoke defect formation. Starting more than 30 years ago, Dawson and Bangham suggested that membrane charge modulates phospholipase activities (Bangham & Dawson, 1959, 1960; Dawson, 1958, 1969). Searching for the cause of PLA_2's anomalous kinetics, Jain et al. (1982) specifically considered the model proposed by Dawson and rejected it

because there was no observed effect of fatty acid alone on the binding of PLA_2 to zwitterionic SUV. Furthermore, fatty acid alone was unable to eliminate the lag time while neutral molecules such as lysolecithin can reduce or eliminate the lag time (Jain & de Haas, 1983; Bell & Biltonen, 1992). Other processes such as conformational changes in PLA_2, covalent modification, oligomerization, and combinations of these have all been proposed to play a role in determining the anomalous kinetics [collated in Bell and Biltonen (1992)]. The rates of these processes were hypothesized to depend on bulk properties of the membrane. However, recognizing that PLA_2's affinity for anionic surfaces is several orders of magnitude greater than for zwitterionic surfaces, Jain and co-workers rejected the more complicated explanations for the anomalous kinetics and returned to Dawson's model and extended its use (Jain et al., 1986a–c, 1988; Jain & Berg, 1989; Berg et al., 1991). The essence of this binding–activation model is that the catalytic rate is dependent primarily on the fraction of PLA_2 bound to the membrane.

The binding–activation model cannot account for all the complex kinetics observed here. The extremely complicated kinetics observed in this work lead us to suggest a litany of membrane properties as modulators of PLA_2 activity: induction of a surface charge, limits on lateral diffusion, microheterogeneities that may result in protein aggregation, compositional phase separation of substrate and reaction product, and large-scale changes in lipid aggregate structure associated with phase separation. These possibilities are among the many which have been previously considered as modulators of membrane-bound enzymes (Kinnunen et al., 1994; Kinnunen, 1991). While it would be convenient to invoke just one mechanism to explain the effect of membrane structure on the function of PLA_2, such parsimony seems inappropriate here. Rather, the analysis of the modulation of PLA_2 activity by synthetic membranes suggests how rich the variety of these effects may be in vivo.

REFERENCES

Apitz-Castro, R., Jain, M. K., & de Haas, G. H. (1982) *Biochim. Biophys. Acta 688*, 349–356.

Bangham, A. D., & Dawson, R. M. C. (1959) *Biochem. J. 72*, 486–492.

Bangham, A. D., & Dawson, R. M. C. (1960) *Biochem. J. 75*, 133–138.

Bell, J. D., & Biltonen, R. L. (1989a) *J. Biol. Chem. 264*, 12194–12200.

Bell, J. D., & Biltonen, R. L. (1989b) *J. Biol. Chem. 264*, 225–230.

Bell, J. D., & Biltonen, R. L. (1992) *J. Biol. Chem. 267*, 11046–11056.

Berg, O. G., Yu, B. Z., Rogers, J., & Jain, M. K. (1991) *Biochemistry 30*, 7283–7297.

Burack, W. R., & Biltonen, R. L. (1994) *Chem. Phys. Lipids 73*, 209–222.

Burack, W. R., Yuan, Q., & Biltonen, R. L. (1993) *Biochemistry 32*, 583–589.

Burack, W. R., Dibble, A., Allietta, M. M., Hoenger, T., & Biltonen, R. L. (1994) *Biophys. J. 66*, A58 (Abstract).

Dawson, R. M. C. (1958) *Biochem. J. 68*, 352–357.

Dawson, R. M. C. (1969) *Methods Enzymol. 14*, 633–648.

Derzko, Z., & Jacobson, K. (1980) *Biochemistry 19*, 6050–6057.

Fernandez, M. S., Mejia, R., & Zavala, E. (1991a) *Biochem. Cell Biol. 69*, 722–727.

Fernandez, M. S., Mejia, R., Zavala, E., & Pacheco, F. (1991b) *Biochem. Cell Biol. 69*, 715–721.

Findlay, E. J., & Barton, P. G. (1978) *Biochemistry 17*, 2400–2405.

Ghomashchi, F., Yu, B. Z., Berg, O. G., Jain, M. K., & Gelb, M. H. (1991) *Biochemistry 30*, 7318–7329.

Grainger, D. W., Reichert, A., Ringsdorf, H., & Salesse, C. (1989) *FEBS Lett. 252*, 73–82.

Grainger, D. W., Reichert, A., Ringsdorf, H., & Salesse, C. (1990) *Biochim. Biophys. Acta 1023*, 365–379.

Hope, M. J., Bally, M. B., Webb, G., & Cullis, P. R. (1985) *Biochim. Biophys. Acta 812*, 55–65.

Jain, M. K., & Apitz-Castro, R. (1978) *J. Biol. Chem. 253*, 7005–7010.

Jain, M. K., & de Haas, G. H. (1983) *Biochim. Biophys. Acta 736*, 157–162.

Jain, M. K., & Berg, O. G. (1989) *Biochim. Biophys. Acta 1002*, 127–156.

Jain, M. K., Egmond, M. R., Verheij, H. M., Apitz-Castro, R., Dijkman, R., & de Haas, G. H. (1982) *Biochim. Biophys. Acta 688*, 341–348.

Jain, M. K., de Haas, G. H., Marecek, J. F., & Ramirez, F. (1986a) *Biochim. Biophys. Acta 860*, 475–483.

Jain, M. K., Rogers, J., Jahagirdar, D. V., Marecek, J. F., & Ramirez, F. (1986b) *Biochim. Biophys. Acta 860*, 435–447.

Jain, M. K., Rogers, J., Marecek, J. F., Ramirez, F., & Eibl, H. (1986c) *Biochim. Biophys. Acta 860*, 462–474.

Jain, M. K., Rogers, J., & de Haas, G. H. (1988) *Biochim. Biophys. Acta 940*, 51–62.

Jain, M. K., Yu, B. Z., & Kozubek, A. (1989) *Biochim. Biophys. Acta 980*, 23–32.

Kinnunen, P. K. (1991) *Chem. Phys. Lipids 57*, 375–399.

Kinnunen, P. K., Koiv, A., Lehtonen, J. Y., Rytomaa, M., & Mustonen, P. (1994) *Chem. Phys. Lipids 73*, 181–207.

Lathrop, B. K., & Biltonen, R. L. (1992) *J. Biol. Chem. 267*, 21425–21431.

Lichtenberg, D., Romero, G., Menashe, M., & Biltonen, R. L. (1986) *J. Biol. Chem. 261*, 5334–5340.

Liscovitch, M., & Cantley, L. C. (1994) *Cell 77*, 329–334.

Maraganore, J. M., Merutka, G., Cho, W., Welches, W., Kezdy, F. J., & Heinrikson, R. L. (1984) *J. Biol. Chem. 259*, 13839–13843.

Marsh, D. (1990) in *CRC Handbook of Lipid Bilayers*, CRC Press, Boca Raton, FL.

Menashe, M., Romero, G., Biltonen, R. L., & Lichtenberg, D. (1986) *J. Biol. Chem. 261*, 5328–5333.

op den Kamp, J. A. F., de Gier, J., & Van Deenen, L. L. (1974) *Biochim. Biophys. Acta 345*, 253–256.

op den Kamp, J. A. F., Kauerz, M., & Van Deenen, L. L. (1975) *Biochim. Biophys. Acta 406*, 169–177.

Roholt, O. A., & Schlamowitz, M. (1961) *Arch. Biochem. Biophys. 94*, 364–379.

Romero, G., Thompson, K., & Biltonen, R. L. (1987) *J. Biol. Chem. 262*, 13476–13482.

Sen, A., Isac, T. V., & Hui, S. W. (1991) *Biochemistry 30*, 4516–4521.

Smaby, J. M., Muderhwa, J. M., & Brockman, H. L. (1994) *Biochemistry 33*, 1915–1922.

Thompson, T. E., Sankaram, M. B., & Biltonen, R. L. (1992) *Comments Mol. Cell. Biophys. 8*, 17–36.

Tinker, D. O., & Wei, J. (1979) *Can. J. Biochem. 57*, 97–106.

Tinker, D. O., Purdon, A. D., Wei, J., & Mason, E. (1978) *Can. J. Biochem. 56*, 552–558.

Upreti, G. C., & Jain, M. K. (1980) *J. Membr. Biol. 55*, 113–121.

Verger, R., Mieras, M. C., & de Haas, G. H. (1973) *J. Biol. Chem. 248*, 4023–4034.

BI951278K